Evaluation of Epipole Estimation Methods with/without Rank-2 Constraint across Algebraic/Geometric Error Functions

Tsuyoshi MIGITA and Takeshi SHAKUNAGA
Okayama University
3-1-1, Tsushima-naka, Okayama, Japan
{migita,shaku}@it.okayama-u.ac.jp

Abstract

The best method for estimating the fundamental matrix and/or the epipole over a given set of point correspondences between two images is a nonlinear minimization, which searches a rank-2 fundamental matrix that minimizes the geometric error cost function. When convenience is preferred to accuracy, we often use a linear approximation method, which searches a rank-3 matrix that minimizes the algebraic error. Although it has been reported that the algebraic error causes very poor results, it is currently thought that the relatively inaccurate results of a linear estimation method are a consequence of neglecting the rank-2 constraint, and not a result of exploiting the algebraic error. However, the reason has not been analyzed fully. In the present paper, we analyze the effects of the cost function selection and the rank-2 constraint based on covariance matrix analyses and show theoretically and experimentally that it is more important to enforce the rank-2 constraint than to minimize the geometric cost function.

1. Introduction

When analyzing a pair of images, the first important step is to estimate its epipolar geometry, or its fundamental matrix, from a set of point correspondences of feature points between images[1, 3, 4, 5, 6, 7, 8, 9, 10]. This estimation problem of epipolar geometry is one of the most important issues in computer vision, and a great number of studies have been performed in an attempt to solve this problem. A highly accurate fundamental matrix is obtained by minimizing the *geometric* cost function (or *Sampson* error), and the resulting fundamental matrix should be bounded to be of rank 2. However, since the rank-2 constraint is difficult to deal with, it is often neglected, or at least relaxed during the main calculation and then considered afterward. In addition, the complexity of the geometric error causes another difficulty in estimating the fundamental matrix. Therefore, we often minimize a linear approximation of the geometric error, i.e., the *algebraic error*. These two approximations result in a linear solution. Although exploitation of the algebraic error function has been criticized in that "algebraic distance has no physical significance [9]," or "linear method does not minimize a physically meaningful quantity [10]," the experimental results presented in [4] indicate that even when the algebraic error function is used, a nearly optimal fundamental matrix can be reconstructed provided that the rank-2 constraint is fully taken into account. However, this consideration has not yet been analyzed in depth. In the present paper, we conduct theoretical and experimental analyses that reveal the reason why the rank-2 constraint is more important than the cost function design for several cases.

Specifically, we analyze four methods arising from the combination of two aspects: constraining the resulting fundamental matrix to be of rank 2 or allowing that of rank 3, and using the geometric error or the algebraic error. We will hereafter refer to these methods as the A2 and A3 methods, and the G2 and G3 methods, respectively. The letters A and G indicate the cost function used, and the numbers 2 and 3 indicate the search space used. For example, the G2 method is a nonlinear minimization method that employs better choices for both aspects (geometric error with rank-2 constraint), and the A3 method employs poorer choices for both aspects (algebraic error without rank-2 constraint). A standard method [4] is to first use the A3 method, with the rank correction, to obtain an initial estimation for the subsequent G2 method. However, since this method suffers from local minima, several researchers recently proposed methods that can produce the globally optimal result [1, 5]. Similarly, the A2 method can be used for globally optimal estimation in the following manner. Since it is a relatively simple rational equation system in the elements of the fundamental matrix or the epipole, it is possible to reduce its minimization to a high-order polynomial equation in only one variable, using a gröbner basis manipulation or a multi-polynomial resultant calculation [2]. This allows us to find

1-4244-1180-7/07/$25.00

all of the solutions, including the global minimum and local solutions[1].

The accuracy of the method is modeled by the covariance matrix of the first-order deviation of the estimation [4, 6, 10]. We derive the covariance matrix for all four methods introduced above. A comparison of these methods reveals the importance of the rank-2 constraint, which has not been fully analyzed previously. In addition, we complete the analyses using some experimental results.

2. Fundamental Matrix Estimation

Here, we formulate a problem of fundamental matrix estimation and define the algebraic/geometric cost functions, as well as the rank-2 constraint.

2.1. Definitions

Consider two perspective cameras and P feature points in a 3-space, and let $\boldsymbol{x}_p$ and $\boldsymbol{x}'_p$ be the homogeneous coordinates of images of the p'th feature point taken by two cameras. Then, the following relation, known as the epipolar constraint [4], holds if the observations are noise-free:

$$\boldsymbol{x}_p'^T F \boldsymbol{x}_p = 0, \tag{1}$$

where F is a *fundamental matrix* that conveys internal and external parameters of the two cameras.

Given a set of feature correspondences $\{(\boldsymbol{x}_p, \boldsymbol{x}'_p)\}$, a standard formulation to estimate F is the minimization of a cost function defined as follows:

$$E(F) := \sum_{p=0}^{P-1} w_p \cdot \left(\boldsymbol{x}_p'^T F \boldsymbol{x}_p\right)^2 , \tag{2}$$

where w_p is the weight for each term. One typical selection is $w_p = 1$ for all p. In this case, the cost function is referred to as an *algebraic* error. Another typical selection is

$$w_p := (|\Pi F \boldsymbol{x}_p|^2 + |\Pi F^T \boldsymbol{x}'_p|^2)^{-1}, \tag{3}$$

$$\text{where } \Pi := \begin{bmatrix} 1 & 0 & 0 \\ 0 & 1 & 0 \end{bmatrix}. \tag{4}$$

The corresponding cost function is called the *geometric* error, which is the sum of the Euclidean distances between the observed feature positions and the corresponding epipolar lines over the two images. Since the geometric error contains F, which is to be estimated, we usually approximate F by the estimation result, and the error is referred to as the *Sampson* error [4, 5, 8]. In the present paper, however, we do not need to strictly distinguish between these two errors.

[1] We have shown in [7] that the A2 method can be reduced to a 1,728th-order polynomial equation in a single variable representing a ratio (such as x/z) of the epipole coordinate (x, y, z).

Although F has 3×3 elements, it has only seven degrees of freedom due to two constraints. First, since the scale of F should not change the optimal F minimizing eq. (2), the search space of F is limited so that its Frobenius norm is 1, hereinafter we write this as $|F|_F^2 = 1$. Second, F should be of rank 2, i.e., there exists a vector $\boldsymbol{e}$ such that $F\boldsymbol{e} = 0$, and $\boldsymbol{e}$ is called an *epipole*.

We use the symbol $\boldsymbol{f}$ to denote a 9-vector containing all elements of the fundamental matrix F, i.e.,

$$\boldsymbol{f} := (a, b, c, d, e, f, g, h, i)^T , \tag{5}$$

$$\text{where } F = \begin{bmatrix} a & b & c \\ d & e & f \\ g & h & i \end{bmatrix}. \tag{6}$$

Then, we can rewrite the epipolar residual $\boldsymbol{x}_p'^T F \boldsymbol{x}_p$ as $(\boldsymbol{x}'_p \otimes \boldsymbol{x}_p)^T \boldsymbol{f}$, where $(a, b, c)^T \otimes (x, y, z)^T := (ax, ay, az, bx, by, bz, cx, cy, cz)^T$. Stacking this residual for each p, we define a P-dimensional residual vector $\boldsymbol{r}$ as

$$\boldsymbol{r} = J\boldsymbol{f} := \begin{bmatrix} \vdots \\ (\boldsymbol{x}'_p \otimes \boldsymbol{x}_p)^T \\ \vdots \end{bmatrix} \boldsymbol{f} \tag{7}$$

where J is a $P \times 9$ Jacobian matrix from $\boldsymbol{f}$ to $\boldsymbol{r}$.

Letting $H = J^T W J$, the cost function eq. (2) is

$$E(\boldsymbol{f}) = \boldsymbol{f}^T H \boldsymbol{f} , \tag{8}$$

where W is a weighting matrix. Basically, the matrix is diagonal and $W = \mathrm{diag}(w_0, w_1, \cdots)$, but it could be any non-negative symmetric matrix. For an estimation problem, H, J, and W are contaminated by noise. However, in the present paper, we analyze the behavior of the solution of a minimization problem around the true solution. Such analyses assume that the true F, H, J, and W are known.

2.2. Several algebraic properties of F

It is useful to introduce the singular value decomposition of F:

$$F = [\boldsymbol{u}_0\ \boldsymbol{u}_1\ \boldsymbol{u}_2] \begin{bmatrix} \varepsilon & & \\ & \sigma_1 & \\ & & \sigma_2 \end{bmatrix} \begin{bmatrix} \boldsymbol{v}_0^T \\ \boldsymbol{v}_1^T \\ \boldsymbol{v}_2^T \end{bmatrix}. \tag{9}$$

Among three singular values of F, let ε be the smallest (the comparison is with respect to absolute values). Ideally $\varepsilon = 0$. Here, $\boldsymbol{v}_0$ is an alias of the previously introduced $\boldsymbol{e}$ (right epipole) when $\varepsilon = 0$, and we also write $\boldsymbol{u}_0$ as $\boldsymbol{e}'$ (left epipole). Note that $\boldsymbol{e}$ (the least significant right singular vector) is also called an epipole, regardless of whether $\varepsilon = 0$. We can easily see that

$$F\boldsymbol{e} = \varepsilon\boldsymbol{e}' , \text{ and } F^T\boldsymbol{e}' = \varepsilon\boldsymbol{e} . \tag{10}$$

For later convenience, let us define

$$B := \begin{bmatrix} \boldsymbol{e} & & \\ & \boldsymbol{e} & \\ & & \boldsymbol{e} \end{bmatrix}, \quad \text{and} \quad \boldsymbol{h}_{3i+j} = \boldsymbol{u}_i \otimes \boldsymbol{v}_j \tag{11}$$

where $(i,j) \in \{0,1,2\}^2$. Nine vectors $\{\boldsymbol{h}_k\}$ form an orthonormal basis for the 9D search space for $\boldsymbol{f}$, and we can write $\boldsymbol{f} = \varepsilon \boldsymbol{h}_0 + \sigma_1 \boldsymbol{h}_4 + \sigma_2 \boldsymbol{h}_8$. This suggests that $\boldsymbol{f}$ should be orthogonal to $\boldsymbol{h}_0$, if the rank-2 constraint is considered ($\varepsilon = 0$). For this reason, we will use $\boldsymbol{h}_0$ extensively, which is abbreviated as $\boldsymbol{h}$.

2.3. Incorporating Rank Constraint

In order to force the resulting matrix to be of rank 2, we extend eq. (8) by adding a penalty term as follows:

$$E_\nu(\boldsymbol{f}) \quad = \quad \boldsymbol{f}^T (H + \nu B B^T) \boldsymbol{f} \,, \tag{12}$$

where $B^T \boldsymbol{f}$ should be 0 if the resulting matrix is exactly rank-2, which is attained when $\nu \to \infty$. And since eq. (10) suggests that $B^T \boldsymbol{f} = \varepsilon \boldsymbol{e}'$, we have $B B^T \boldsymbol{f} = \varepsilon \boldsymbol{h}$ and $\varepsilon = \boldsymbol{e}'^T B^T \boldsymbol{f} = \boldsymbol{h}^T \boldsymbol{f}$. Therefore, the matrix B in the above equation can be replaced by the vector $\boldsymbol{h}$ as follows:

$$E_\nu(\boldsymbol{f}) \quad = \quad \boldsymbol{f}^T (H + \nu \boldsymbol{h}\boldsymbol{h}^T) \boldsymbol{f} \,. \tag{13}$$

Minimization of this function under the constraint $|F|_F^2 = 1$ reduces to the following eigen-equation as $\nu \to \infty$:

$$\left(H + \nu \boldsymbol{h}\boldsymbol{h}^T - \lambda I \right) \boldsymbol{f} = 0 \,. \tag{14}$$

In the following sections, we analyze the behavior of the estimation result around the true solution for the methods that minimize the geometric/algebraic error with/without rank-2 constraint. Note that the behavior is not affected by the actual implementation and/or the parameterization.

Here, let us focus on the case of $W = I$ and $\nu \to \infty$ (the A2 method that employs the *algebraic* error *with* the rank-2 constraint). The present analyses will show how well the A2 method approximates the optimal G2 method (*geometric* error *with* rank-2 constraint) and the degree to which the A2 method is better than the A3 or G3 methods (algebraic/geometric error *without* rank-2 constraint).

To analyze the behavior of the solution of eq. (14), we have to consider the 'inverse' of $(H + \nu \boldsymbol{h}\boldsymbol{h}^T)$ as $\nu \to \infty$, which we write by a † operator defined as follows:

$$H^\dagger \quad := \quad H^- - \frac{H^- \boldsymbol{h}\boldsymbol{h}^T H^-}{\boldsymbol{h}^T H^- \boldsymbol{h}} \,, \tag{15}$$

which is based on the following identity, similar to the Sherman-Morrison inversion formula:

$$\left(H^- - \frac{H^- \boldsymbol{h}\boldsymbol{h}^T H^-}{\nu^{-1} + \boldsymbol{h}^T H^- \boldsymbol{h}} \right) \left(H + \nu \boldsymbol{h}\boldsymbol{h}^T \right) = H^- H \,,$$

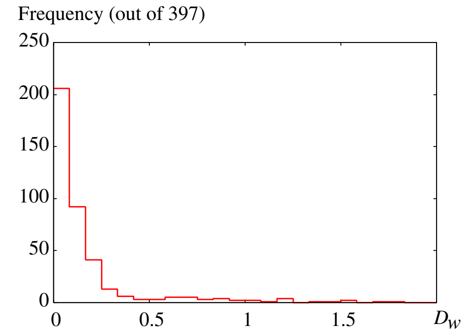

Figure 1. Histogram of the standard deviation of w_p^{-1} for 397 image pairs among 36 images.

where H^- denotes the Moore-Penrose generalized inverse of H. The † is defined by limiting $\nu \to \infty$ in this formula. The † has similar properties to the usual generalized inverse, but the rank-2 constraint is fully taken into account. Compare the following properties:

$$H^\dagger \boldsymbol{f} = 0 \,, \quad H^\dagger H H^\dagger = H^\dagger \,, \quad H^\dagger \boldsymbol{h} = 0 \,, \tag{16}$$

$$H^- \boldsymbol{f} = 0 \,, \quad H^- H H^- = H^- \,, \quad H^- \boldsymbol{h} \neq 0 \,. \tag{17}$$

2.4. Properties of w_p^{-1}

In the case for the algebraic error, we assume that $w_p = 1$. Although this is a seemingly crude approximation, experimental results (Fig. 1) show that, for a lot of cases, the actual w_p of eq. (3) is compactly distributed around 1, and so letting $w_p = 1$ is indeed a good approximation. For each image pair, we let D_w be the standard deviation of w_p^{-1} divided by the mean of w_p^{-1}. The figure shows a histogram of D_w over 397 image pairs from 36 images, four examples of which are shown in Fig. 3. We can see that D_w is small. Specifically, D_w is less than 0.1 for more than half (over 200 out of 397) of the image pairs. We will show that the cost function selection affects the estimation accuracy by $O(D_w^2)$ and is much smaller than the degradation caused by neglecting the rank-2 constraint. Note that, theoretically, if the cameras that are used are affine, then the w_p's are exactly same for all p's, and we often use near-affine views for epipolar geometry estimation.

3. Covariance Matrix as Accuracy Measure

We need a criterion to discuss which method is 'better' or 'worse.' The analysis in the following section is based on a standard theory [4, 6, 10] of accuracy measure using the covariance matrix of the first-order variation of the solution of a given estimation method. For discussing a covariance matrix in Section 3.2 and the following sections, we need to first introduce the first-order variation in Section 3.1.

For the following discussion, we assume the coordinates $\boldsymbol{x}_p$'s and $\boldsymbol{x}'_p$'s are noise-free, and thus the epipolar residuals are all zero, i.e., $\boldsymbol{r} = 0$. Noise components are explicitly indicated by a Δ symbol or other designated symbols. Let us define a noise-free input vector $\boldsymbol{x}^T := (\cdots (\Pi \boldsymbol{x}_p)^T \; (\Pi \boldsymbol{x}'_p)^T \cdots)^T$, and a small noise vector $\boldsymbol{d}^T := (\cdots (\Pi \Delta \boldsymbol{x}_p)^T \; (\Pi \Delta \boldsymbol{x}'_p)^T \cdots)^T$. When an input vector is polluted by a noise like $\boldsymbol{x} + \boldsymbol{d}$, then the residual $\boldsymbol{r}$ changes to $\boldsymbol{r} + \Delta \boldsymbol{r}$. Similarly, $\boldsymbol{f}$ changes to $\boldsymbol{f} + \Delta \boldsymbol{f}$, and $\boldsymbol{e}$ changes to $\boldsymbol{e} + \Delta \boldsymbol{e}$. We will express these Δ-values as a function of $\boldsymbol{d}$ to the first order. Then, we will derive covariance matrices such as $\mathcal{E}[(\Delta \boldsymbol{f})(\Delta \boldsymbol{f})^T]$, where $\mathcal{E}[\cdot]$ is the expectation operator. Since $\boldsymbol{d}$ is a vector having a geometric dimension, we assume $\mathcal{E}[\boldsymbol{d}\boldsymbol{d}^T] = \epsilon^2 I$, where ϵ is called a *noise level*. Although we can develop a similar theory for an arbitrary $\mathcal{E}[\boldsymbol{d}\boldsymbol{d}^T]$, we prefer to simplify the present discussion.

3.1. First-order Analysis around the True Solution

The deviation $\Delta \boldsymbol{r}$ is expanded as

$$\Delta \boldsymbol{r} = \Delta J \boldsymbol{f} + J \Delta \boldsymbol{f} \tag{18}$$

$$= M^T \boldsymbol{d} + J \Delta \boldsymbol{f} \tag{19}$$

where

$$M^T := \begin{bmatrix} \ddots & & \\ & (\Pi F^T \boldsymbol{x}'_p)^T \; (\Pi F \boldsymbol{x}_p)^T & \\ & & \ddots \end{bmatrix}, \tag{20}$$

and M^T is a $P \times 4P$ Jacobian matrix from $\boldsymbol{d}$ to $\boldsymbol{r}$, which consists of P diagonal blocks of size 1×4.

Then, the cost function eq. (2) can be rewritten as

$$(\Delta \boldsymbol{r})^T W (\Delta \boldsymbol{r}) \tag{21}$$

More precisely, this is an approximation used in Gauss-Newton iteration for nonlinear optimization, where second-order derivatives are neglected, and it is also sufficient for the present analysis, because $\boldsymbol{d}$ is small.

Fundamental matrix estimation based on the minimization of eq. (2) can be regarded as the minimization of eq. (21) over $\Delta \boldsymbol{f}$, where $\Delta \boldsymbol{f}$ is the displacement between the estimated matrix and the true matrix. Ideally, $\Delta \boldsymbol{f}$ should be 0, which means that the true $\boldsymbol{f}$ is obtained. However, $\Delta \boldsymbol{f}$ cannot be 0 for a general $\boldsymbol{d}$.

Next, let us explicitly derive $\Delta \boldsymbol{f}$ based on eq. (21). If the rank-2 constraint is neglected, we have to minimize $(M^T \boldsymbol{d} + J \Delta \boldsymbol{f})^T W (M^T \boldsymbol{d} + J \Delta \boldsymbol{f})$, which reduces to $J^T W (M^T \boldsymbol{d} + J \Delta \boldsymbol{f}) = 0$, so the solution is

$$\Delta \boldsymbol{f} = -(J^T W J)^- J^T W M^T \boldsymbol{d}\,. \tag{22}$$

If the rank-2 constraint is taken into account, then we have to consider the first-order variation of eq. (14):

$$((\Delta H) + \nu((\Delta \boldsymbol{h})\boldsymbol{h}^T + \boldsymbol{h}(\Delta \boldsymbol{h})^T) - (\Delta \lambda) I)\boldsymbol{f} + (H + \nu \boldsymbol{h}\boldsymbol{h}^T - \lambda I)(\Delta \boldsymbol{f}) = 0\,. \tag{23}$$

From this equation, $\Delta \boldsymbol{f}$ is obtained as

$$\Delta \boldsymbol{f} = -H^\dagger J^T W M^T \boldsymbol{d}. \tag{24}$$

Note that $H^- = (J^T W J)^-$ in the previous result is replaced by $H^\dagger$.

3.2. Comparing the Covariance Matrices

Here, $\Delta \boldsymbol{f}$ is a first-order approximation of the estimation error caused by an additive noise $\boldsymbol{d}$ on the input. In addition, since $\Delta \boldsymbol{f}$ is a linear function of $\boldsymbol{d}$, it is also a zero-mean. In other words, the estimation is unbiased to the first order. Thus, the covariance matrix of $\Delta \boldsymbol{f}$ is $\mathcal{E}[(\Delta \boldsymbol{f})(\Delta \boldsymbol{f})^T]$. The covariance matrix for the rank-2-constrained estimation is as follows:

$$V(W) := \epsilon^2 H^\dagger J^T W M^T M W J H^\dagger, \tag{25}$$

which is straightforwardly derived from eq. (24). The covariance matrix is denoted by $V(W)$ because it is a function of W. The covariance matrix defines an ellipsoid $(\Delta \boldsymbol{f})^T V(W)^- (\Delta \boldsymbol{f}) < \theta$, and the probability that $\Delta \boldsymbol{f}$ falls into the ellipsoid is determined by θ, which is not a function of W.

Let us assume, for two covariance matrices A and B, that $\boldsymbol{a}^T A^- \boldsymbol{a} < \boldsymbol{a}^T B^- \boldsymbol{a}$ holds for any $\boldsymbol{a}$, then the ellipsoid of B is completely subsumed by that of A. In this case, we can safely say that the method yielding the covariance matrix B is better than the method yielding A. The inequality is equivalent to $\boldsymbol{a}^T A \boldsymbol{a} > \boldsymbol{a}^T B \boldsymbol{a}$ and is also written as $A \succ B$ [6], which means that $A - B$ is a positive matrix.

4. Covariance Matrix of $\Delta \boldsymbol{f}$ and $\Delta \boldsymbol{e}$

Here, we compare the covariance matrices of $\Delta \boldsymbol{f}$ and $\Delta \boldsymbol{e}$, for the A2, A3, G2, and G3 methods. We will demonstrate that the rank-2 constraint is more important than the cost function selection for many cases.

4.1. Distribution of $\Delta \boldsymbol{f}$ using geometric error

When the fundamental matrix is estimated by the best method (G2, which uses the geometric error with rank-2 constraint), the corresponding covariance matrix is obtained by substituting $W = (M^T M)^{-1}$ into eq. (25), yielding

$$V_{G2} := \epsilon^2 H^\dagger. \tag{26}$$

If the rank-2 constraint is neglected, then the corresponding covariance matrix is easily calculated from eq. (22) as follows:

$$V_{G3} := \epsilon^2 H^-. \tag{27}$$

Then, the difference is

$$V_{G3} - V_{G2} = \epsilon^2 \frac{H^- \boldsymbol{h}\boldsymbol{h}^T H^-}{\boldsymbol{h}^T H^- \boldsymbol{h}}. \tag{28}$$

Table 1. Four covariance matrices of $\Delta \boldsymbol{f}$

Cost function \ Search space	Rank-2	Rank-3
Geometric	A	$A+B$
Algebraic	$A+O(\epsilon^2 D_w^2)$	$A+B+O(\epsilon^2 D_w^2)$

where $\begin{cases} B = \epsilon^2 \dfrac{H^- \boldsymbol{h}\boldsymbol{h}^T H^-}{\boldsymbol{h}^T H^- \boldsymbol{h}} \\ A = \epsilon^2 H^\dagger \end{cases}$

This difference is a positive matrix. It proves qualitatively that the estimation is more accurate when the rank-2 constraint is enforced. However, this shows nothing quantitatively. Therefore, we complete the discussion using some experimental results in a later section of the present paper.

4.2. Distribution of $\Delta \boldsymbol{f}$ using algebraic error

The algebraic error is regarded as an approximated geometric error, where W is replaced by $W + \Delta W$. More specifically, $\Delta W = I - W$ with $W = \mu(M^T M)^{-1}$, where μ is a scalar that adjusts the mean of the elements of W to be 1, and μ does not affect the estimation results. The elements of ΔW are $O(D_w)$. In the following, we still use the symbol H to refer to $J^T W J$.

With the rank-2 constraint, the $\Delta \boldsymbol{f}$ estimated by the odd weight $W + \Delta W$ is

$$\begin{aligned} \Delta \boldsymbol{f} &= \left(H + J^T \Delta W J\right)^\dagger J^T (W + \Delta W) M^T \boldsymbol{d} \qquad (29)\\ &= \left(H^\dagger - H^\dagger J^T \Delta W J H^\dagger\right) J^T (W + \Delta W) M^T \boldsymbol{d} \\ &\quad + O(\epsilon D_w^2) \qquad (30) \end{aligned}$$

where we used the following approximation:

$$(H + J^T \Delta W J)^\dagger \approx H^\dagger - H^\dagger \left(J^T \Delta W J\right) H^\dagger, \qquad (31)$$

which can be verified directly.

Here, $\Delta \boldsymbol{f}$ is a zero-mean, and the covariance matrix is

$$\begin{aligned} V_{A2} = \epsilon^2 &\left(H^\dagger - H^\dagger J^T \Delta W J H^\dagger\right) J^T (W + \Delta W) M^T M \cdot \\ &(W + \Delta W) J \left(H^\dagger - H^\dagger J^T \Delta W J H^\dagger\right) + O(\epsilon^2 D_w^2) \\ = \; &\epsilon^2 \left(H^\dagger - H^\dagger J^T \Delta W J H^\dagger\right) (H + 2J^T (\Delta W) J) \cdot \\ &\left(H^\dagger - H^\dagger J^T \Delta W J H^\dagger\right) + O(\epsilon^2 D_w^2) \\ = \; &\epsilon^2 H^\dagger + O(\epsilon^2 D_w^2) \qquad (32) \end{aligned}$$

where we used

$$\begin{aligned} &(W + \Delta W) W^{-1} (W + \Delta W) \\ = \; &W + 2(\Delta W) + (\Delta W) W^{-1} (\Delta W). \qquad (33) \end{aligned}$$

In eq. (32), it is important that the first-order terms of ΔW cancel each other out. Consequently, this differs from eq. (26), where the optimal W is used, by only $O(\epsilon^2 D_w^2)$. Similarly, the covariance matrix using the algebraic error without the rank-2 constraint is as follows:

$$V_{A3} = \epsilon^2 H^- + O(\epsilon^2 D_w^2) \, . \qquad (34)$$

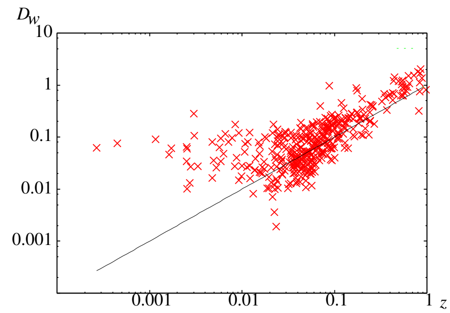

Figure 2. Relationship between the standard deviation of w_p^{-1} and the z-coordinate of the epipole

4.3. Comparison of the covariance matrices for $\boldsymbol{f}$

The results are summarized in Table 1, where $A = \epsilon^2 H^\dagger$ (eq. (26)) is equivalent to the (KCR-) lower bound [6], and $B = \epsilon^2 H^- \boldsymbol{h}\boldsymbol{h}^T H^- / (\boldsymbol{h}^T H^- \boldsymbol{h})$ (eq. (28)) is a corruption caused by removing the rank-2 constraint, whereas using the algebraic error rather than the geometric error causes a corruption of $O(\epsilon^2 D_w^2)$, which we do not have to distinguish with $O(D_w^2)$ because the leading term of a covariance matrix is $O(\epsilon^2)$. The lower-right algorithm is the linear A3 algorithm.

Although the actual magnitude of D_w is a complicated function, which is not easy to deal with, the experimental results shown in Fig. 1 show that D_w is very small for a lot of cases. Another important property of D_w is shown in Fig. 2, where D_w's are plotted with respect to the z-coordinates of the epipoles, and we can see that D_w and the z-coordinate have a strong correlation. Thus, the z-coordinate is a good measure for the D_w, and the difficulty of the estimation is determined by the distance between the epipole and the image center or the infinite point. This agrees with an observation reported in [8] whereby forward/backward motion estimation is more difficult than sideways-motion estimation. We can assume that for several applications epipoles are nearer to an infinite point than to the image center. In such cases, the z is small, as is D_w. As a result, the $O(D_w^2)$ terms are considerably smaller than B. Thus, the rank-2 constraint is more important than the cost function selection. In other words, the algebraic error is sufficiently accurate, and well comparable to the geometric error, when the rank-2 constraint is fully taken into account. This explains the experimental results in [4, Fig. 10.3].

These discussions assume that we know the true $\boldsymbol{f}$ when we estimate $\boldsymbol{f}$. This is, however, impossible in practice.

Table 2. Four covariance matrices of $\Delta\boldsymbol{e}$

Cost function \ Search space	Rank-2	Rank-3
Geometric	A	$A+B$
Algebraic	$A+O(\epsilon^2 D_w^2)$	$A+B+O(\epsilon^2 D_w^2)$

where $\begin{cases} B = \epsilon^2 K \dfrac{H^- \boldsymbol{h}\boldsymbol{h}^T H^-}{\boldsymbol{h}^T H^- \boldsymbol{h}} K^T \\ A = \epsilon^2 K H^\dagger K^T \end{cases}$

We can only know an approximation of $\boldsymbol{f}$ or other related entities, such as epipoles. Since the approximation error is of the first-order, its effects appear in second-order terms in $\Delta\boldsymbol{f}$. Thus, the previously described first-order terms are not affected and are valid for the case with unknown $\boldsymbol{f}$.

4.4. Distribution of Δe

Since $\boldsymbol{e}$ is determined by the equation $F\boldsymbol{e} = 0$, its first-order deviation is calculated by the perturbation theory of eigenvectors [6], and the result is as follows:

$$\Delta\boldsymbol{e} \quad = \quad -K\Delta\boldsymbol{f} \quad \text{where} \quad K := F^- B^T, \qquad (35)$$

and F^- is the generalized inverse of F, thus K has the following singular value decomposition:

$$K \quad = \quad [\boldsymbol{v}_1, \boldsymbol{v}_2]\mathrm{diag}(\sigma_1^{-1}, \sigma_2^{-1})[\boldsymbol{h}_3, \boldsymbol{h}_6]^T. \qquad (36)$$

As is for $\Delta\boldsymbol{f}$, $\boldsymbol{e}$ is zero-mean to the first order, and its covariance matrix is described by

$$KVK^T \qquad (37)$$

where V is the covariance matrix of $\Delta\boldsymbol{f}$ for all four cases discussed previously. In addition, the covariance matrix for $\boldsymbol{e}$ is rank-2. The results are also summarized in Table 2. The only difference from Table 1 is that all covariance matrices are multiplied from the left by K and from the right by K^T.

Note that, although the rank correction based on singular value decomposition [3], which is usually employed after the A3 method, may improve F significantly, it does not change $\boldsymbol{e}$, which is defined in Section 2.2 as the right singular vector of F. Thus, for $\Delta\boldsymbol{e}$, the right-lower entry of Table 2 applies to the 8-point algorithm regardless of whether the rank correction is performed.

5. Experiment

We present some experimental results over a real image set, consisting of 36 images, including those shown in Fig. 3. In the figures, epipolar lines are also shown when the leftmost two images and the rightmost two images are paired. Thirty images out of 36 are taken from a circular trajectory around the object, and six additional images are added in order to increase the variation of the epipole position. In total, there are 100 feature points, which are tracked manually. These coordinates are 'normalized' [3] to be zero-mean, and to have a unit covariance matrix. There are 630 possible pairs and 397 pairs contain seven or more, at most 51, corresponding points. Note that there are 16 pairs that have only seven correspondences, and we cannot apply those methods without rank-2 constraint to such pairs. For the number of correspondences, the mean is 20.2 and the standard deviation is 10.9.

Since we do not know the ground truth, we modify the input data so that the epipolar constraints are satisfied. For this purpose, we first obtain the fundamental matrix minimizing the Sampson error, then the point coordinates are corrected by regarding the Sampson-error-minimized fundamental matrix as the ground truth. We use such a pseudo-real data set because it better represents the point distribution of a real situation, compared to relying on an entirely numerical simulations.

The first example is the left pair in Fig. 3, and the results are shown in Table 3, where two nontrivial eigenvalues of the covariance matrices for $\Delta\boldsymbol{e}$ are shown. These values can be considered as the squared uncertainty radius of the estimated epipole along the principal axes, and thus a smaller value is preferred.

The degradation caused by neglecting the rank-2 constraint is approximately $(2.8\ 0.03)$ for both cost functions, and the degradation caused by employing the algebraic error is of the order of $(0.001, 0.001)$ regardless of the rank-2 constraint. Figure 4 shows the ellipses generated by these four covariance matrices. The ellipses form two groups, and the inner group consists of ellipses with the rank-2 constraint. The selection of the cost function causes no visible difference.

Table 4 shows another example, based on the rightmost pair of Fig. 3, where the rank-2 constraint has a $(5, 0)$ effect, while the cost-function-caused effects are much smaller. Figure 5 shows the ellipses generated by these four covariance matrices. Here, the ellipses again form two groups, and the rank constraint has a non-negligible effect for these cases.

For more general analyses, let us define a degradation index as the ratio of the difference of the degraded and true eigenvalues divided by the true eigenvalue. We focus on the larger eigenvalue representing the long axis of the ellipse. For example, in Table 3, the index for rank-caused degradation is (4.081-1.261)/1.261=2.23. For Table 4, the index is (6.120-0.949)/0.949 = 5.449. Larger values indicate greater degradations. Figure 6 shows histograms over 397 image pairs, for rank-caused and cost-function-caused degradation indices. The rank-caused degradation (left curve) is 0.0001 through 0.01 for most cases, while the cost-function-caused degradation (right curve) is 0.01 through 10 for most cases. Thus, the rank constraint is shown to be more important

Figure 3. Examples of the images (0th, 5th, 10th, and 19th images out of 36 images), with the epipolar lines superimposed.

Table 3. Example 1: Covariance matrices of Δe, 0th and 5th images, with 36 correspondences

Cost function \ Search space	Rank-2	Rank-3
Geometric	(1.261 0.512)	(4.081 0.546)
Algebraic	(1.262 0.513)	(4.083 0.546)

Figure 4. Ellipses of Table 3.

Table 4. Example 2: Covariance matrices of Δe, 10th and 19th images, with 13 correspondences

Cost function \ Search space	Rank-2	Rank-3
Geometric	(0.949 0.294)	(6.120 0.380)
Algebraic	(0.954 0.295)	(6.167 0.381)

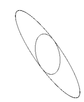

Figure 5. Ellipses of Table 4.

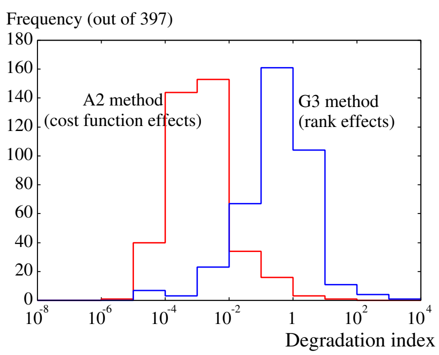

Figure 6. Histograms of the degradation indices over 397 images. Seven point cases are excluded for the method without rank-2 constraint.

than the cost function selection.

6. Conclusions

For epipolar geometry estimation, we herein analyzed the importance of the rank-2 constraint, as well as that of the selection of the geometric/algebraic cost function, and demonstrated through qualitative and quantitative analyses that the former is more important than the latter.

Future areas for examination include further analyses on D_w, the theoretical behavior of which we did not discuss in the present paper, and analyses of the estimation errors with respect to the second order.

This work has been supported in part by a Grant-In-Aid for Scientific Research (No.15300062) from the Ministry of Education, Science, Sports, and Culture of Japan.

References

[1] G. Chesi and A. Garulli. Estimating the fundamental matrix via constrained least-squares: A convex approach. *IEEE Trans. on Pattern Analysis and Machine Intelligence*, 24(3):397–401, 2002.

[2] D. Cox, J. B. Little, and D. O'Shea. *Using Algebraic Geometry*. Springer, 1998.

[3] R. I. Hartley. In defence of the 8-point algorithm. *IEEE Trans. on Pattern Analysis and Machine Intelligence*, 19(6):580–593, 1997.

[4] R. I. Hartley and A. Zisserman. *Multiple View Geometry in Computer Vision*. Cambridge University Press, 2004.

[5] F. Kahl and D. Henrion. Globally optimal estimates for geometric reconstruction problems. In *International Conference on Computer Vision*, pages 978–985. Beijing, China, 2005.

[6] K. Kanatani. *Statistical Optimization for Geometric Computation*. Elsevier, 1996.

[7] T. Migita and T. Shakunaga. One-dimensional search for reliable epipole estimation. In *IEEE Pacific-Rim Symposium on Image and Video Technology*, pages 1215–1224. Taiwan, 2006.

[8] J. Oliensis. Exact two-image structure from motion. *IEEE Trans. on Pattern Analysis and Machine Intelligence*, 24(12):1618–1633, 2002.

[9] P. Torr and D. Murray. The development and comparison of robust methods for estimating the fundamental matrix. *Intl. J. of Computer Vision*, 24(3):271–300, 1997.

[10] Z. Zhang. Determining the epipolar geometry and its uncertainty: A review. *Intl. J. of Computer Vision*, 27(2):161–198, 1998.